Numerical Heat Transfer, Part A, 47: 549–569, 2005

ISSN: 1040-7782 print/1521-0634 online
DOI: 10.1080/10407780590891236

Taylor & Francis
Taylor & Francis Group

NONLINEAR ANALYSIS OF RUBBER-BASED POLYMERIC MATERIALS WITH THERMAL RELAXATION MODELS

R. V. N. Melnik
Mathematical Modelling and Computational Sciences, Wilfrid Laurier University, Waterloo, Ontario, Canada

D. V. Strunin and A. J. Roberts
Department of Mathematics and Computing, University of Southern Queensland, Australia

Using mathematical modeling and computer simulation, nonlinear dynamics of rubber-based polymers has been studied with due regard for the effect of thermal relaxation. Main results have been obtained for the case of elongational oscillations of a ring-shaped body subjected to periodic ("internal") boundary conditions. Particular emphasis has been placed on high-frequency and short spatial variations of temperature and displacement, in which the role of nonlinearities in the dynamics of the material and their close connection with the effect of thermal relaxation time can be best appreciated. It is shown how the vanishing relaxation time can lead to an attenuation of nonlinear effects in the thermomechanical system.

1. INTRODUCTION

The effect of thermal relaxation in rubber-based polymers is one of the characteristics that render them different from "hard" solids. In idealized solids, thermal energy is transported by quantized electronic excitations (free electrons) and by the quanta of lattice vibrations (phonons). A relaxation time appears naturally as the characteristic of thermal resistance in the solid, due to dissipative collisions of these quanta. Such thermal resistance is more markedly pronounced in such materials as rubber-based polymers, which are important in a wide range of applications [1].

Thermal relaxation is responsible for finite speed of heat propagation. This effect is also known as the "second sound" or the hyperbolic effect, due to the type of the equation governing heat propagation [2–5].

Most contributions to the rigorous analysis of coupled thermomechanical fields in thermoelasticity theory have traditionally been devoted to linear models (see [6] and references therein). Rubber-based polymers provide a classical example in which nonlinear effects are essential in the adequate description of the material dynamics. Using the phenomenology of these materials [7, 8], only few recent articles

Received 22 December 2003; accepted 15 September 2004.
This research was supported by Australian Research Council Grant 179406. We thank anonymous referees for constructive comments accounted for in the final version of the manuscript.
Address correspondence to R. V. N. Melnik, Mathematical Modelling and Computational Sciences, Wilfrid Laurier University, 75 University Ave W, Waterloo, ON N2L 3C5, Canada. E-mail: rmelnik@wlu.ca

NOMENCLATURE

$\mathbf{B}$	Finger (left Cauchy-Green) strain tensor ($=\mathbf{V}^2 \equiv \mathbf{F}\mathbf{F}^T$)	$\mathbf{Q}$	rigid body rotation (an orthogonal tensor)
$\tilde{c}$	heat capacity	R	gas constant per mole
c_{ijkl}	elastic coefficients tensor	$\mathbf{S}$	second Piola-Kirchhoff stress
$\mathbf{C}$	Cauchy (right Cauchy-Green) strain tensor ($=\mathbf{U}^2 \equiv \mathbf{F}^T\mathbf{F}$)	$\mathbf{T}$	Cauchy (true) stress tensor
$\mathbf{D}$	displacement gradient ($=\nabla\mathbf{u} \equiv \mathbf{F} - \mathbf{I}$)	$\mathbf{u}$	displacement vector
D_i	penalty for imposing the incompressibility constrain	$\mathbf{U}$	positive-definite symmetric matrix
$\bar{\mathbf{D}}(\mathbf{v})$	deformation rate tensor $[=\mathrm{sym}(\dot{\mathbf{F}}\mathbf{F}^{-1}) = \frac{1}{2}(\nabla\mathbf{v} + \nabla\mathbf{v}^T)]$	$\mathbf{v}$	velocity vector
e	internal energy (per unit volume)	$\mathbf{V}$	positive-definite symmetric matrix
e_1^0	internal (equilibrium) energy part at the reference temperature	$\mathbf{x}$	original (undeformed) configuration of the body
$\mathbf{E}$	Green (Green-Lagrange-St.Venant) strain tensor $[=\frac{1}{2}(\mathbf{D} + \mathbf{D}^T + \mathbf{D}^T\mathbf{D}) = \frac{1}{2}(\mathbf{F}^T\mathbf{F} - \mathbf{I})]$	$\mathbf{y}$	deformed configuration of the body
		α_j	material-dependent constants
		α_0	thermal expansion coefficient
		β_{jk}	elements of the thermoelastic pressure matrix
		ΔS	total entropy of deformation
$\mathbf{f}_0$	applied volumetric body force	ϵ_{jk}	components of the strain tensor
$\mathbf{F}$	deformation gradient [$= \mathbf{QU} = \mathbf{VQ}$]	θ_0	absolute temperature
$\mathbf{F}_1$	density of the applied volumetric body force	$\mathbf{\Lambda}$	set of independent variables
		μ_j	material-dependent constants
F_2	heat density	ρ	mass density of the material
$g(J)$	given function	$\boldsymbol{\sigma}$	nominal stress tensor that measures force per unit area in the reference configuration
$g(\theta)$	shear moduli-related function		
G	shear modulus		
$\mathbf{I}$	second-order identity tensor	$\boldsymbol{\sigma}^T$	first Piola-Kirchhoff stress tensor ($=J\mathbf{T}\hat{\mathbf{F}}$)
k	bulk modulus		
$\tilde{k}_g$	ground-state bulk modulus in pure dilatation	τ_0	thermal relaxation time
		ψ	free-energy function
$\mathcal{K}$	heat conduction coefficient	ψ_e	elastic part of the free-energy function
M_c	(number average) chain molecular weight	ψ_{vol}	volumetric part of the free-energy function
N	constant		
$\mathbf{q}$	heat flux	ψ_1^0	free energy at the temperature θ_0

discuss numerical results obtained for these materials with general nonlinear models of thermoelasticity (see [9–12] and references therein). Nonlinearities in the dynamics of rubber-based polymers are closely interwoven with the effect of second sound.

So far there have been no attempts to employ hyperbolic models to study nonlinear thermoelasticity. In order to bridge this gap, our aim in this article is to explore a combined effect of nonlinearity and thermal relaxation time in rubber-based polymers.

To simplify mathematical analysis, we consider elongational oscillations of a ring-shaped body (Figure 1) made of the rubber-based polymeric material. An experimental setup for the problem can be thought of in the following way. The elastic ring is put inside a circular tube with rigid walls. It is assumed that the tube is lubricated from inside and that friction between the polymeric solid material and the tube walls is negligible. When the material is undisturbed, there is no gap between the rubber-based polymer and the walls. Initial local heating will cause a (local) expansion of the rubber-based polymer, with its particles having the freedom

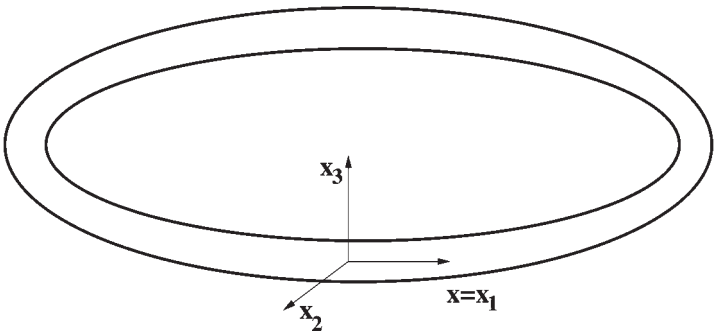

Figure 1. Ring-shaped structure made of a rubber-based polymeric material.

to move only along the tube. As a result, one-dimensional thermoelastic waves will start propagating, with volume changes forced by the rigid walls.

This setup gives an example of the dynamics that is attractive from a physical point of view and is convenient to study numerically. Indeed, the ring, regarded as a one-dimensional structure, has no ends and therefore is not subjected to externally imposed boundary conditions at the ends (while spatial periodicity with the period equal to the ring's perimeter can be viewed as an "internal" boundary condition). This property makes the ring an ideal model object for studying intrinsic dynamics of coupled thermomechanical systems. Furthermore, it is important that for systems with such a topology we can effectively employ a relatively simple Fourier decomposition approach which automatically guarantees the periodicity of the unknown fields.

The article is organized as follows. In Section 2 we formulate basic balance equations governing the dynamics of the material and complement them by constitutive relations. In Section 3 we specify the free-energy function, allowing for the volumetric contributions and coupled thermomechanical effects. Section 4 is devoted to a model of elongational oscillations of a ring-shaped structure. The interactions between nonlinear oscillations of the structure, induced by thermomechanical coupling, and the thermal relaxation time are demonstrated by numerical examples in Section 5.

2. BALANCE EQUATIONS AND CONSTITUTIVE RELATIONS

We assume that the motion of the rubber-based polymer material is governed by the kinematic laws,

$$\mathbf{y} = \mathbf{x} + \mathbf{u}(\mathbf{x}, t) \tag{2.1}$$

where $\mathbf{x} = (x_1, x_2, x_3)$ is the original and $\mathbf{y} = (y_1, y_2, y_3)$ is the deformed configuration of the body, and $\mathbf{u} = (u_1(\mathbf{x}), u_2(\mathbf{x}), u_3(\mathbf{x}))$ is the displacement vector. The motion at each point of the body can be represented by the deformation gradient,

$$\mathbf{F} = \left[\frac{\partial y_i}{\partial x_j}\right]_{i,j=1,2,3} = \mathbf{I} + \frac{\partial \mathbf{u}}{\partial \mathbf{x}} \tag{2.2}$$

where $\mathbf{I}$ is the second-order identity tensor. Further, let ρ be the mass density of the material, e be the internal energy (per unit volume), $\mathbf{T}$ be the Cauchy (true) stress tensor that measures the contact force per unit area in the deformed configuration, $\mathbf{v}$ be the velocity vector, $\mathbf{q}$ be the heat flux, $\mathbf{F}_1 = \rho\mathbf{f}_0$ be the density of the applied volumetric body force $\mathbf{f}_0$, and F_2 be the heat density (all measured in the body current configuration). Then, the evolution of a thermoelastic body can be described by a coupled system consisting of three balance equations, for linear momentum, mass, and energy, which in the Eulerian (spatial) formulation has the form (see [13], p. 18, e.g.)

$$\begin{cases} \rho\dot{\mathbf{v}} = \operatorname{div}\mathbf{T} + \mathbf{F}_1, \qquad \dot{\rho} + \rho\operatorname{div}\mathbf{v} = 0 \\ \rho\dot{e} - \mathbf{T}:\bar{\mathbf{D}}(\mathbf{v}) + \operatorname{div}\mathbf{q} = F_2 \end{cases} \tag{2.3}$$

where all physical quantities are regarded as functions of $\mathbf{y}$ and t. The Eulerian formulation (2.3) can be a starting point for the development of a model based exclusively on the Finger tensor as a strain measure (see, for example, [9]), which then can allow us to compute thermoelastic moduli directly in terms of this tensor. Our approach here is different and is based on dealing with the general nonlinear Green (Green-Lagrange-St.Venant) strain tensor $\mathbf{E} = \left[\epsilon_{ij}\right]_{i,j=1,2,3}$ defined in terms of the displacement gradient $\mathbf{D}$ (see the Nomenclature for details). We assume the linearized form of $\mathbf{E}$ given by $\frac{1}{2}(\nabla\mathbf{u} + \nabla\mathbf{u}^T)$ with the corresponding deformation rate tensor $\bar{\mathbf{D}}(\mathbf{v})$. As usual, by $\dot{\mathbf{v}}$ in (2.3) we denote the material time derivative of $\mathbf{v}$ defined as $\dot{\mathbf{a}} = \partial\mathbf{a}/\partial t + \mathbf{v}\cdot\nabla\mathbf{a}$, where the expression on the left is computed at fixed $\mathbf{x}$, while the expression on the right is computed at fixed $\mathbf{y}$. In what follows we use the dot notation for both frameworks, and the velocity function is always written as $\mathbf{v} = \dot{\mathbf{y}}$. The dyadic operations are defined in the standard way (e.g., [14]) as $\mathbf{a}\cdot\mathbf{b} = \sum_{m,n=1}^{3} e_m\left[\sum_{i=1}^{3} a_{mi}b_{in}\right]e_n^T$ and $\mathbf{a}:\mathbf{b} = |\mathbf{a}\cdot\mathbf{b}|$, $|c| = \sum_{m=1}^{3} c_{mm}$ for single- and double-dot products for Cartesian tensors, respectively.

Since $\mathbf{T}$ measures force per unit area in the present (deformed) configuration of the body, the use of $\mathbf{T}$ in the Eulerian setting is most natural [15]. However, in compressible applications of thermoelasticity theory the assumption of isochoric (or volume-preserving) deformations, $J \equiv \det\mathbf{F} = 1$, can be violated locally. This gives us a good practical reason to transform the system (2.3) to another form. This transformation involves the multiplication of balance equations for momentum and energy by J and the use of the Lagrangian form of the balance-of-mass equation [9, 11, 16]. The resulting equations are written then in terms of the weighted Cauchy tensor (the Kirchhoff stress) $\hat{\mathbf{T}} = J\mathbf{T}$. Note that in this formulation $\dot{\mathbf{F}} = \nabla_{\mathbf{x}}\mathbf{v}$.

Since under constraints like those described in the Introduction the rubber-based polymers and other complex solid polymers exhibit volume changes [17–19], it is practical to reformulate model (2.3) in the equivalent Lagrangian (referential) form that will be used for our analysis in the subsequent discussion:

$$\begin{cases} \rho_0\ddot{\mathbf{y}} = \operatorname{div}\boldsymbol{\sigma} + \rho_0\mathbf{f}_0 \qquad \rho = J^{-1}\rho_0 \\ \rho_0\dot{e} - \boldsymbol{\sigma}^T:(\nabla\mathbf{v}) + \rho_0\operatorname{div}\mathbf{q} = F_2 \end{cases} \tag{2.4}$$

where $\boldsymbol{\sigma} = J\hat{\mathbf{F}}^T\mathbf{T}$ is the (generally not symmetric) nominal stress tensor that measures force per unit area in the reference configuration, $\hat{\mathbf{F}} = (\mathbf{F}^T)^{-1}$. Note also that $\boldsymbol{\sigma}\mathbf{F}^T = \mathbf{F}\boldsymbol{\sigma}^T \Longleftrightarrow$ the symmetry of $\mathbf{T} = J^{-1}\mathbf{F}\boldsymbol{\sigma}$.

The next step in the model formulation is to refine constitutive relationships, including stress–strain and strain energy applied to modeling the behavior of rubber-based polymeric materials. In a standard manner, the volume-preserving part of the strain energy function is approximated in terms of the three principal semiaxes of the strain ellipsoid (or simply, extension ratios $\lambda_i, i = 1, 2, 3$, corresponding to principal stretches) by assuming that the initial state (x_0, y_0, z_0) is deformed via the affine deformation $x = \lambda_1 x_0, \quad y = \lambda_2 y_0, \quad z = \lambda_3 z_0$. Mathematically, the squares of these extension ratios can be defined as the eigenvalues of the Finger $\mathbf{C}$ (or Cauchy $\mathbf{B}$) strain tensor, e.g., [12, 16]. If we further assume that there is no change of internal energy during deformation, we can define the elastic property of rubber-based polymeric materials in the Gaussian region by the strain-energy relation that follows from the standard thermodynamic analysis (e.g., [7], p. 65),

$$\psi_e(\mathbf{E}) = \theta_0 \, \Delta S = \frac{1}{2} G \sum_{i=1}^{3} (\lambda_i^2 - 1) \tag{2.5}$$

where ΔS is the total entropy of deformation, ψ_e is the elastic part of the free-energy function per unit volume of the material, and θ_0 is the absolute temperature. The shear modulus, G, in (2.5) is defined by $G = Nk\theta_0 = \rho R\theta_0 / M_c$, where k is the bulk modulus, R is the gas constant per mole, N is the number of chains per unit volume, M_c is the (number average) chain molecular weight. The above expression for the elastic part of the free-energy function has been derived under isothermal conditions [7, 12] and strictly speaking can be applied to reversible isothermal processes only. Note that in this case the stress–strain relation is given by $\mathbf{S} = 2\rho_0 \partial \psi_e / \partial \mathbf{C} = \rho_0 \partial \psi_e / \partial \mathbf{E}$, with $\mathbf{S}$ being the second Piola-Kirchhoff stress that is connected to the Cauchy stress tensor by the standard relationship (e.g., [12, 16, 20]). The above relation, exact for the isothermal and isentropic processes, defines hyperelastic (or Green elastic) materials as opposed to Cauchy elastic materials that have a nonconservative structure (e.g., [8], p. 176). The Cauchy stress for hyperelastic materials is given by $\mathbf{T} = \rho(\partial \psi_e / \partial \mathbf{F})\mathbf{F}^T$, where the derivative is taken for fixed temperature θ (see [12], p. 64; [16], and [21], p. 266). This is used in the Eulerian formulation (2.3) discussed above (recall that $\mathbf{S} = J\mathbf{F}^{-1}\mathbf{T}\hat{\mathbf{F}} \Longleftrightarrow \mathbf{T} = J^{-1}\mathbf{F}\mathbf{S}\mathbf{F}^T$). However, taking into account that $\mathbf{F}(\partial \psi_e / \partial \mathbf{E}) = \partial \psi_e / \partial \mathbf{F} = (\partial \psi_e / \partial \mathbf{E})\mathbf{F}^T$, we get the expression for the nominal stress that we use in our computations with the model (2.4) (e.g., [8], p. 153), $\boldsymbol{\sigma} = \rho_0(\partial \psi_e / \partial \mathbf{E})\mathbf{F}^T \equiv \rho_0 H(\mathbf{F})$, where the nominal stress is understood as the elastic response function $H(\mathbf{F})$ of a material under consideration. Rubber-based polymericmaterials provide a prime example in which such a response is essentially nonlinear. Due to the nonlinearity, in the general case (2.5) has to be corrected to allow for the non-Gaussian chain statistics. Many authors use the standard Mooney correction of the elastic part of the free energy, ψ_e. The main disadvantage of this approach is that by using such a representation [as well as (2.5)] for the elastic part of the free-energy function, it is difficult to separate isochoric (deviatoric) and volumetric contributions. An alternative representation of the volume-preserving part of the strain-energy function [$\psi_e(\mathbf{E})$] is given in terms of the strain invariants of right- or left-modified Cauchy-Green tensor $\bar{\mathbf{C}} = J^{-2/3}\mathbf{C}$ and $\bar{\mathbf{B}} = J^{-2/3}\mathbf{B}$, respectively, that is, $\bar{I}_1 = \sum_{i=1}^{3} \bar{\lambda}_i^2$ and $\bar{I}_2 = \sum_{i=1}^{3} \bar{\lambda}_i^{-2}$, where $\bar{\lambda}_i = J^{-1/3}\lambda_i, i = 1, 2, 3$, are the eigenvalues of $\bar{\mathbf{C}}$, known as the modified principal deviatoric stretches, which satisfy the standard incompressibility condition $\prod_{i=1}^{3} \bar{\lambda}_i = 1$ [12, 16]. Then the elastic part of

the free-energy function can be given in the Rivlin form $\psi_e = \sum_{i,j=0}^{N} C_{ij}(\bar{I}_1 - 3)^i (\bar{I}_2 - 3)^j$, $C_{00} = 0$, which describes Mooney-Rivlin materials when $N = 1$ (as well as neo-Hookean materials when, in addition, $C_{01} = 0$). Unfortunately, in the general case the elastic part of the free-energy function represented in the above form cannot be decoupled in the principal directions, and therefore fails to satisfy the Valanis-Landel hypothesis requiring separability of the strain-energy function, $\psi_e = \Sigma_{i=1}^{3} w(\bar{\lambda}_i)$. A theoretical justification of this condition is provided by the Taylor expansion of ψ_e near the isochoric pure dilatation $\bar{\lambda}_i = 1$ in $\bar{\lambda}_i - 1$. It can be shown (see [8], p. 494) that, up to the fifth order, ψ_e can be represented in a separable form. In this article we use the Ogden form of the strain-energy function, which automatically satisfies the Valanis-Landel hypothesis:

$$\psi_e = \sum_{i=1}^{3} \sum_{j=1}^{N} \frac{\mu_j}{\alpha_j} \left(\bar{\lambda}_i^{\alpha_i} - 1 \right) \tag{2.6}$$

where $N \geq 3$, μ_j, α_j, $j = 1, \ldots, N$, are material-dependent constants. We note that the expression (2.6) (and other approximations of the elastic part of the free-energy function discussed above) does not allow automatically for thermal effects. However, these effects are critical for rubber-based polymeric materials, and the dependence of constitutive relation on temperature will be a subject of our discussion in the next section.

3. APPROXIMATIONS OF THE FREE-ENERGY FUNCTION

There are two important issues to be discussed in this section. First, for the rubber-based material under constraints, which we consider in this article, the volumetric contribution is essential. In this case, one of the typical assumptions imposed on the free-energy function is its decoupled structure, which is often taken for granted in the literature in the context of numerical experiments conducted for rubber-like materials [22–25]. However, it is known that in the general case the free-energy function cannot be split as a pure sum of two components, one due to shear (elastic part) and the other due to volume change (see, e.g., [8, 12] and references therein). In fact, the idea of coupling between the two components was originally motivated by experimental works that go back to the early 1970s (e.g., [26]), when it was shown that at large enough extensions the strain energy for rubber-based materials cannot be expressed as a sum of the above two parts. Therefore, in the general case a proper inclusion of volumetric contributions into the free-energy function is a nontrivial task.

Second, as we mentioned before, the stress–strain relation discussed in the previous section remains, in essence, uncoupled with the temperature field of the material. We emphasize, however, that the thermomechanical coupling is a key phenomenon for rubber-based polymeric materials, and uncoupled models may lead to misleading results in computing the dynamic behavior of these materials.

3.1. Allowing for Volumetric Contributions

Formally, for an arbitrary dilatation parameter $\epsilon = J - 1$, we can take into account the volumetric part of the free-energy function by splitting the free-energy function into distortional and dilatational components,[1]

$$\psi_e(\bar{\lambda}_1, \bar{\lambda}_2, J) = \psi_e(\bar{\lambda}_1, \bar{\lambda}_2, 1) + \epsilon \frac{\partial \psi_e}{\partial J} + k_g \tilde{g}(J) \tag{3.1}$$

where $\tilde{k}_g$ is the ground-state bulk modulus in pure dilatation (i.e., where $\bar{\lambda}_1 = \bar{\lambda}_2 = 1$), and $g(J)$ is a function chosen from the consistency conditions with the classical theory (see [8], p. 518). Note that the case of $J = 1$ is a particular case of $J = \theta$ with $\theta > 0$ and $\theta \to 1$ (e.g., [25]). Since the dilatation parameter is typically small in the context of rubber-like polymeric materials most widely used in applications ($\sim 10^{-4}$), this function can often be chosen as identically zero and the decomposition of the motion into a volume-preserving distortional part and a dilatational part can be simplified. Indeed, in this case the dilatation effect can be well approximated by the following expansion (typically the first two terms will do the job):

$$\psi_e(\bar{\lambda}_1, \bar{\lambda}_2, J) = \sum_{i=0}^{\infty} \epsilon^i \frac{\partial \psi_e}{\partial J}(\bar{\lambda}_1, \bar{\lambda}_2, 1) \tag{3.2}$$

Unfortunately, as we mentioned earlier, in the general case the free-energy function cannot be represented as a simple sum of its volumetric and isochoric components. Below we explain how the coupling between these two components can be taken into account.

3.2. Thermomechanical Coupling via the Free-energy Function

We effectively couple volumetric and isochoric parts of the free-energy function by introducing a coupling factor $f(J, \theta)$ [12],

$$\psi(\bar{\mathbf{E}}, \theta) = \psi_{\text{vol}}(J, \theta) + f(J, \theta)\psi_{\text{iso}}(\bar{\mathbf{E}}, \theta) \tag{3.3}$$

where we use a new notation, ψ, for the free-energy function (instead of the old one, ψ_e) to reflect its dependency on temperature. Note that energy functions dependent on both the deformation gradient and the temperature are used frequently in the literature, but at the computational level most authors assume that $f = 1$, which may not always be appropriate (e.g., [12, 26]) in the analysis of rubber-based materials. The volumetric part of the free-energy function is determined via the penalty arguments $\psi_{\text{vol}} = \sum_{i=1}^{N} D_i \tilde{f}_i(J, \theta)$, with D_i being interpreted as a penalty for imposing the incompressibility constrain. Specific choices of functions $\tilde{f}_i$ for rubber-based materials have been analyzed in the literature by various authors (e.g., [12, 16, 25]). Here by setting $\theta = \theta_0$ (which should lead to $\psi_{\text{vol}} = 0$ due to a choice of $\tilde{f}_i$) and $f = 1$ representation (3.3) is reduced to the classical incompressible case where $\psi_{\text{iso}} = \psi_e \equiv \psi$ is a function of $\bar{\lambda}_i, i = 1, 2, 3$ only. In the general case, however,

[1]Recall that in the decomposition of the strain $\mathbf{E} = \mathbf{E}^* + 1/3[\text{tr}(\mathbf{E})]\mathbf{I}$, $\mathbf{E}^*$ is called the distortional part of the strain and $\text{tr}\,\mathbf{E}$ is the dilatational part (e.g. [8], p. 348).

function ψ_{iso} is dependent on both strain $\bar{\mathbf{E}}$ and temperature θ and is represented as a sum of two parts, equilibrium, ψ_1, and nonequilibrium, ψ_2,

$$\psi_{\text{iso}}(\bar{\mathbf{E}}, \theta) = \psi_1 + \psi_2 \tag{3.4}$$

Then, according to [11, 22], we can postulate that

$$\psi_i = \delta_i \psi_i^0 - \beta_{jk}\epsilon_{jk}(\theta - \theta_0) + e_i^0\left(1 - \frac{\theta}{\theta_0}\right) \qquad i = 1, 2;\ j, k = 1, 2, 3 \tag{3.5}$$

where e_1^0 is the internal (equilibrium) energy part at the reference temperature θ_0, ψ_1^0 is the free-energy at the temperature θ_0, ϵ_{jk} are components of the strain tensor $\mathbf{E}$, and β_{jk} are elements of the thermoelastic pressure matrix (in the linear case, it is the matrix product between the matrix of elastic moduli and the thermal expansion matrix). Using arguments of [9] (see also p. 366 in [11]), in our work we set $\psi_2 = 0$. In this case the resulting free-energy function is an analog of the Taylor expansion of the Helmholtz free-energy function in the vicinity of the natural state ($\epsilon_{ij} = 0$ and $\theta = \theta_0$) in the classical linear theory of thermoelasticity [27],

$$\psi(\bar{\mathbf{E}}, \theta) = \psi(0, \theta_0) + \frac{1}{2}c_{ijkl}\epsilon_{ij}\epsilon_{kl} - \beta_{ij}\epsilon_{ij}(\theta - \theta_0) - \frac{\tilde{c}(\theta - \theta_0)^2}{2\theta_0} \tag{3.6}$$

where $\tilde{c}$ is the heat capacity and c_{ijkl} is the elastic coefficients tensor. Note that the third term in (3.6) is the thermomechanical coupling term. Finally, we note that for computational experiments reported in Section 5, the volumetric part of the free-energy function in (3.3) is chosen as $\psi_{\text{vol}} = \bar{c}(\theta - \theta_0 - \theta \log \theta/\theta_0)$, where $\bar{c}$ is the rigid heat capacity [9]. Having the free-energy function, the internal energy (per unit reference volume) is determined via the entropy, η, in the standard manner as

$$e = \psi + \theta\eta \qquad \eta = -\frac{\partial \psi}{\partial \theta} \tag{3.7}$$

The general form of the free-energy function brings appropriate corrections to the stress–strain relation. Recall that since ψ_e is just an isothermal part of the free-energy function, the stress–strain relation can be "exact" only for isentropic (η is kept constant) or isothermal (θ is kept constant) processes. In the context of entropy-elastic materials, we have to cover a more general case, hence we refine these approximations as follows:

$$\boldsymbol{\sigma} = \boldsymbol{\sigma}(\Lambda, \bar{\mathbf{D}}) \qquad \text{and as a special case} \qquad \boldsymbol{\sigma} = \rho_0 \frac{\partial \psi}{\partial \mathbf{F}} \quad \text{or} \quad \mathbf{S} = \rho_0 \frac{\partial \psi}{\partial \mathbf{E}} \tag{3.8}$$

where Λ is a set of independent variables chosen for the adequate description of material behavior and such that the entropy inequality is satisfied (see Section 5.3 in [21] for details). The free-energy function (per unit reference volume), ψ, in (3.13) is determined by (3.3).

We do not consider here viscous and rheological effects, although such effects may become detectable in rubber-like polymeric materials when impulse diffuses

through the material in the process of microscopic motion of particles. The reader can consult [11, 21, 28] on the existing procedures for how such effects can be incorporated. In what follows, the main focus will be on the effect of thermal relaxation and its influence on the nonlinear dynamics of the thermomechanical system. This effect is introduced into our model by the Cattaneo-Vernotte (CV) equation (e.g., [29, 30]),

$$\tau_0 \dot{\mathbf{q}} + \mathbf{q} = -\mathcal{K}\nabla\theta \tag{3.9}$$

where $\mathbf{q}$ is the heat flux, $\mathcal{K}$ is the heat conduction coefficient, and τ_0 is the thermal relaxation time. This equation evolves into the standard Fourier law, $\mathbf{q} = -\mathcal{K}\nabla\theta$, in the limit of vanishing relaxation time $\tau_0 \to 0^+$.

Finally, we note that the model described in this section may be enhanced to include rheological effects. This can readily be handled with known procedures (e.g., [11]).

4. ELONGATIONAL OSCILLATIONS OF A RING-SHAPED STRUCTURE

The definition of the strain according to formula (2.2) (and ultimately, the definition of the free-energy function) requires the specification of kinematic laws (2.1). As soon as such laws are specified for the rubber-based polymeric material, we can perform the analysis of nonhomogeneous situations, in which the strains may vary from point to point in the deformed body.

Given experimental evidence of the importance of volumetric changes in rubber-based materials [17–19], it is instructive to consider an example in which the deviation of the material from incompressible conditions is allowed. The ring-shaped structure described in the Introduction is curved, so that solid particles are moved along curved trajectories. If, however, the radius of the ring is sufficiently large while the displacements of the particles are small, their trajectories can be well approximated by straight lines. We therefore can use Cartesian coordinates for the analysis of the one-dimensional elongational motion of the ring defined by the kinematics

$$y_1 = x_1 + u(x_1, t) \qquad y_2 = x_2,\ y_3 = x_3 \tag{4.1}$$

In this case, the coordinate $x \equiv x_1$ is directed along the ring, while coordinates x_2 and x_3 are directed across the ring. It must be emphasized that this motion can be exhibited in compressible materials only. The law (4.1) is clearly different from that of the elongational motion under near-incompressibility conditions [15], for example, $y_1 = x + u(x,t),\ y_2 = x_2/\sqrt{1 + u_x(x,t)},\ y_3 = x_3/\sqrt{1 + u_x(x,t)}$.

For the kinematic law (4.1), the deformation gradient (2.2) is defined by the diagonal matrix $\mathbf{F} = \mathrm{diag}(1 + \partial u/\partial x, 1, 1)$ where we set $x_1 \equiv x$ to simplify notation. Hence, the Finger strain tensor has the form $\mathbf{B} = \mathrm{diag}((1 + \partial u/\partial x)^2, 1, 1)$ which provides us with three eigenvalues denoted further as $\lambda_1 = \lambda_2 = 1,\ \lambda_3 = (1 + \partial u/\partial x)^2$. Therefore, J as a function of $\partial u/\partial x$, and modified principal deviatoric stretches can be represented in the form

$$J = 1 + \frac{\partial u}{\partial x} \qquad \bar{\lambda}_{1,2} = J^{-1/3} \qquad \bar{\lambda}_3 = \left(1 + \frac{\partial u}{\partial x}\right)^2 J^{-1/3} \tag{4.2}$$

As rubber-based polymers may exhibit large deformations, in principle the energy and other functions should be taken in the general forms suitable for both small and large deformations. Since in this section we focus only on the case of small perturbations, these general forms can be reduced to simpler ones by decomposing them into Taylor series in $\partial u/\partial x$ and $(\theta - \theta_0)$. Indeed, substituting (4.2) into ψ_1^0 and retaining only linear and quadratic terms in the Taylor series, we get

$$\psi_1^0 = \frac{1}{2}\sum_{i=1}^{3} \mu_i \frac{\partial u}{\partial x} + \frac{1}{8}\left[\sum_{i=1}^{3} \mu_i(3\alpha_i - 2) + 4k_0\right]\left(\frac{\partial u}{\partial x}\right)^2 + \cdots \tag{4.3}$$

Under the assumption of Section 3.2 the remaining terms in the free-energy function (3.3) turn into zero when $\theta = \theta_0$. Referring to [31], we note that for $u \equiv 0$ there should be no internal stresses ($\sigma \equiv 0$). Hence, due to (3.13), we conclude that linear terms should be absent in the expansion of ψ_1^0, and therefore $\sum_{i=1}^{3} \mu_i = 0$. Further, we note that for the available data for many rubber-like polymers [11, 32] $4k_0$ is typically a dominant term in the square brackets of (4.3). This immediately simplifies the relation (4.4) to

$$\psi_1^0 \approx \frac{k_0}{2}\left(\frac{\partial u}{\partial x}\right)^2 \tag{4.4}$$

Then we take the shear-moli-related function $g(\theta) = b(\theta/\theta_0)^a + d$ in the simplest form corresponding to $a = 0$. In this case $dg/d\theta = 0$ and consequently we have

$$\delta_1 = \frac{\theta}{\theta_0} \tag{4.5}$$

Substituting (4.5) and (4.4) into (3.5) for $i = 1$ and replacing β_{jk} by a scalar β, we obtain

$$\psi_1 \approx \frac{\theta}{2\theta_0} k_0 \left(\frac{\partial u}{\partial x}\right)^2 - \beta(\theta - \theta_0)\frac{\partial u}{\partial x} + k_0\alpha_0\theta_0\left(1 - \frac{\theta}{\theta_0}\right)\frac{\partial u}{\partial x} \tag{4.6}$$

In view of (3.4) and $\psi_2 = 0$, the formula (4.6) also represents the function ψ_{iso}. Inserting (4.6) and the expression for ψ_{vol} (see Section 3) into (3.3), in which we assume for simplicity that $f(\theta) = 1$, yields the function ψ:

$$\psi = \bar{c}\left(\theta - \theta_0 - \theta \log\frac{\theta}{\theta_0}\right) + \frac{\theta}{2\theta_0} k_0 \left(\frac{\partial u}{\partial x}\right)^2 - (\beta + k_0\alpha_0)(\theta - \theta_0)\frac{\partial u}{\partial x} \tag{4.7}$$

Expression (4.7) can be simplified further by decomposing $\log(\theta/\theta_0)$ into Taylor series in small value $(\theta - \theta_0)/\theta_0$:

$$\log\frac{\theta}{\theta_0}=\log\left(1+\frac{\theta-\theta_0}{\theta_0}\right)\approx\frac{\theta-\theta_0}{\theta_0}-\frac{1}{2}\left(\frac{\theta-\theta_0}{\theta_0}\right)^2 \tag{4.8}$$

Substituting (4.8) into (4.7) reduces the latter to the form

$$\psi=-\frac{\bar{c}}{2}\frac{(\theta-\theta_0)^2}{\theta_0}+\frac{\theta}{2\theta_0}k_0\left(\frac{\partial u}{\partial x}\right)^2-\gamma(\theta-\theta_0)\frac{\partial u}{\partial x} \tag{4.9}$$

where

$$\gamma=\beta+k_0\alpha_0$$

The stress is readily determined by differentiating (4.9) with respect to $\partial u/\partial x$:

$$\sigma=\rho_0\frac{\theta}{\theta_0}k_0\frac{\partial u}{\partial x}-\rho_0\gamma(\theta-\theta_0) \tag{4.10}$$

The energy e is determined from (3.7) with the help of (4.9):

$$e=-\frac{\bar{c}}{2}\frac{(\theta-\theta_0)^2}{\theta_0}+\frac{\bar{c}}{\theta_0}(\theta-\theta_0)\theta+\gamma\theta_0\frac{\partial u}{\partial x} \tag{4.11}$$

from which

$$\dot{e}=-\frac{\bar{c}}{\theta_0}(\theta-\theta_0)\dot{\theta}+\frac{\bar{c}}{\theta_0}\dot{\theta}(2\theta-\theta_0)+\gamma\theta_0\frac{\partial\dot{u}}{\partial x} \tag{4.12}$$

We note that the first term on the right-hand side of (4.12) contains the small multiplier $(\theta-\theta_0)/\theta_0$. Disregarding this term, we get

$$\dot{e}=\frac{\bar{c}}{\theta_0}(2\theta-\theta_0)\dot{\theta}+\gamma\theta_0\frac{\partial\dot{u}}{\partial x}\approx\bar{c}\dot{\theta}+\gamma\theta_0\frac{\partial\dot{u}}{\partial x} \tag{4.13}$$

Using (4.10) we have

$$\sigma^T:(\nabla\mathbf{v})=\rho_0\frac{k_0}{\theta_0}\theta\frac{\partial u}{\partial x}\frac{\partial\dot{u}}{\partial x}-\rho_0\gamma(\theta-\theta_0)\frac{\partial\dot{u}}{\partial x} \tag{4.14}$$

Now we are in a position to rewrite the momentum and energy balance equations (2.4) using (4.10), (4.13), and (4.14). Together with the Cattaneo-Vernotte (CV) equation they have the form

$$\begin{cases}\rho_0\ddot{u}=\dfrac{k_0}{\theta_0}\theta\dfrac{\partial^2u}{\partial x^2}+\dfrac{k_0}{\theta_0}\dfrac{\partial\theta}{\partial x}\dfrac{\partial u}{\partial x}-\gamma\dfrac{\partial\theta}{\partial x}\\ \bar{c}\dot{\theta}=-\dfrac{\partial q}{\partial x}+\dfrac{k_0}{\theta_0}\theta\dfrac{\partial u}{\partial x}\dfrac{\partial\dot{u}}{\partial x}-\gamma(\theta-\theta_0)\dfrac{\partial\dot{u}}{\partial x}\\ \tau_0\dfrac{\partial q}{\partial t}+q=-\mathcal{K}\dfrac{\partial\theta}{\partial x}\end{cases} \tag{4.15}$$

The heat flux q can be excluded from (4.15) in a straightforward manner by (1) differentiating the CV equation with respect to x, which leads to

$$\tau_0 \frac{\partial}{\partial t}\left(\frac{\partial q}{\partial x}\right) + \frac{\partial q}{\partial x} = -\mathcal{K}\frac{\partial^2 \theta}{\partial x^2}$$

and (2) substituting therein the derivative $\partial q/\partial x$ extracted from the energy equation. Doing so, we obtain

$$\begin{cases} \rho_0 \ddot{u} = \dfrac{k_0}{\theta_0}\theta\dfrac{\partial^2 u}{\partial x^2} + \dfrac{k_0}{\theta_0}\dfrac{\partial \theta}{\partial x}\dfrac{\partial u}{\partial x} - \gamma\dfrac{\partial \theta}{\partial x} \\ \tau_0 \bar{c}\ddot{\theta} + \bar{c}\dot{\theta} = \mathcal{K}\dfrac{\partial^2 \theta}{\partial x^2} + \tau_0 k_0\left[\left(\dfrac{\partial \dot{u}}{\partial x}\right)^2 + \dfrac{\partial u}{\partial x}\dfrac{\partial \ddot{u}}{\partial x}\right] + k_0\dfrac{\partial u}{\partial x}\dfrac{\partial \dot{u}}{\partial x} \\ \qquad\qquad -\gamma\tau_0\dot{\theta}\dfrac{\partial \dot{u}}{\partial x} - \gamma\tau_0\theta\dfrac{\partial \ddot{u}}{\partial x} - \gamma\theta\dfrac{\partial \dot{u}}{\partial x} \end{cases} \tag{4.16}$$

Finally, we substitute the expression for $\ddot{u}$ from the momentum equation [in (4.16)] into the energy equation, replace θ for $\theta_0 + T$ ($T = \theta - \theta_0$), and retain only linear and quadratic terms in T and u:

$$\begin{cases} \rho_0 \ddot{u} = k_0\dfrac{\partial^2 u}{\partial x^2} - \gamma\dfrac{\partial T}{\partial x} + \dfrac{k_0}{\theta_0}\dfrac{\partial T}{\partial x}\dfrac{\partial u}{\partial x} + \dfrac{k_0}{\theta_0}T\dfrac{\partial^2 u}{\partial x^2} \\ \tau_0 \bar{c}\ddot{T} + \bar{c}\dot{T} = \left(\mathcal{K} + \tau_0\dfrac{\gamma^2\theta_0}{\rho_0}\right)\dfrac{\partial^2 T}{\partial x^2} - \tau_0\dfrac{\gamma k_0\theta_0}{\rho_0}\dfrac{\partial^3 u}{\partial x^3} \\ \qquad - \gamma\theta_0\dfrac{\partial \dot{u}}{\partial x} + \tau_0 k_0\left(\dfrac{\partial \dot{u}}{\partial x}\right)^2 - \tau_0\dfrac{2\gamma k_0}{\rho_0}T\dfrac{\partial^3 u}{\partial x^3} \\ \qquad - \tau_0\dfrac{2\gamma k_0}{\rho_0}\dfrac{\partial T}{\partial x}\dfrac{\partial^2 u}{\partial x^2} - \tau_0\dfrac{2\gamma k_0}{\rho_0}\dfrac{\partial^2 T}{\partial x^2}\dfrac{\partial u}{\partial x} + \tau_0\dfrac{\gamma^2}{\rho_0}T\dfrac{\partial^2 T}{\partial x^2} + \tau_0\dfrac{k_0^2}{\rho_0}\dfrac{\partial u}{\partial x}\dfrac{\partial^3 u}{\partial x^3} \\ \qquad + k_0\dfrac{\partial \dot{u}}{\partial x}\dfrac{\partial u}{\partial x} - \tau_0\gamma\dot{T}\dfrac{\partial \dot{u}}{\partial x} - \gamma T\dfrac{\partial \dot{u}}{\partial x} \end{cases} \tag{4.17}$$

It is easy to see that the linearized version of (4.17) coincides with the linear Lord-Shulman model of hyperbolic thermoelasticity [33]. In this sense, the system (4.17) can be viewed as a generalization of the classical Lord-Schulman theory to nonlinear hyperbolic thermoelasticity [5]. All quantities of the model (4.18) can be nondimensionalized using appropriate combinations of the dimensional parameters with independent dimensionalities. We have seven dimensional parameters in the model:

$$\begin{array}{llll} \rho_0(\mathrm{g/cm^3}) & k_0(\mathrm{g/cm\,s^2}) & \theta_0\,(\mathrm{K}) & \mathcal{K}(\mathrm{g\,cm/s^3\,K}) \\ \gamma(\mathrm{g/cm\,s^2\,K}) & \tau_0\,(\mathrm{s}) & \bar{c}(\mathrm{g/cm\,s^2\,K}) & \end{array} \tag{4.18}$$

In (4.19) there are only four parameters with independent dimensionalities, and using $(\rho_0, k_0, \theta_0, \mathcal{K})$ as those, we obtain the following dimensional scales:

$$x_* = \frac{\rho_0^{1/2}\mathcal{K}\theta_0}{k_0^{3/2}} \qquad t_* = \frac{\rho_0\mathcal{K}\theta_0}{k_0^2} \qquad T_* = \theta_0 \tag{4.19}$$

Omitting algebraic rearrangements, we write the nondimensional system in which,

for simplicity, we use the same variables' notations as above:

$$\begin{cases} \ddot{u} = \dfrac{\partial^2 u}{\partial x^2} - \dfrac{C}{B}\dfrac{\partial T}{\partial x} + \dfrac{\partial T}{\partial x}\dfrac{\partial u}{\partial x} + T\dfrac{\partial^2 u}{\partial x^2} \\ A\ddot{T} + \dot{T} = \left(B + \dfrac{AC^2}{B}\right)\dfrac{\partial^2 T}{\partial x^2} - AC\dfrac{\partial^3 u}{\partial x^3} - C\dfrac{\partial \dot{u}}{\partial x} + AB\left(\dfrac{\partial \dot{u}}{\partial x}\right)^2 \\ \qquad -2AC\,T\dfrac{\partial^3 u}{\partial x^3} - 2AC\dfrac{\partial T}{\partial x}\dfrac{\partial^2 u}{\partial x^2} - 2AC\dfrac{\partial^2 T}{\partial x^2}\dfrac{\partial u}{\partial x} + \dfrac{AC^2}{B}T\dfrac{\partial^2 T}{\partial x^2} \\ \qquad +AB\dfrac{\partial u}{\partial x}\dfrac{\partial^3 u}{\partial x^3} + B\dfrac{\partial \dot{u}}{\partial x}\dfrac{\partial u}{\partial x} - AC\,\dot{T}\dfrac{\partial \dot{u}}{\partial x} - C\,T\dfrac{\partial \dot{u}}{\partial x} \end{cases} \tag{4.20}$$

and

$$A = \frac{\tau_0 k_0^2}{\rho_0 \mathcal{K} \theta_0} \qquad B = \frac{k_0}{\theta_0 \bar{c}} \qquad C = \frac{\gamma}{\bar{c}}$$

In the ring-shaped body of the perimeter L, the thermomechanical fields are spatially periodic, with the period L linked to the basis wave number $k = 2\pi/L$. We introduce fields of velocity and rate of temperature change, $v = \partial u/\partial t, q = \partial T/\partial t$, and seek the solution to (4.21) in the form of a Fourier series:

$$\begin{aligned} u &= \sum_{n=-\infty}^{\infty} U_n(t)e^{ink x} \qquad v = \sum_{n=-\infty}^{\infty} V_n(t)e^{ink x} \\ T &= \sum_{n=-\infty}^{\infty} T_n(t)e^{ink x} \qquad q = \sum_{n=-\infty}^{\infty} Q_n(t)e^{ink x} \end{aligned} \tag{4.21}$$

Substituting (4.21) into (4.20) and equating coefficients near $\exp(ink_0 x)$ leads to an infinite system of coupled ordinary differential equations for the Fourier amplitudes:

$$\begin{cases} \dfrac{dU_n}{dt} = V_n \\ \dfrac{dV_n}{dt} = -(nk)^2 U_n - \dfrac{C}{B}ink T_n \\ \qquad -k^2 \sum\limits_{m=-\infty}^{\infty} m(n-m)T_m U_{n-m} - k^2 \sum\limits_{m=-\infty}^{\infty} m^2 U_m T_{n-m} \\ \dfrac{dT_n}{dt} = Q_n \\ \dfrac{A\,dQ_n}{dt} = -Q_n - \left(B + \dfrac{AC^2}{B}\right)(nk)^2 T_n + ACi(nk)^3 U_n - Cink V_n \\ \qquad -ABk^2 \sum\limits_{m=-\infty}^{\infty} m(n-m)V_m V_{n-m} + 2ACik^3 \sum\limits_{m=-\infty}^{\infty} m^3 U_m T_{n-m} \\ \qquad +2ACik^3 \sum\limits_{m=-\infty}^{\infty} m(n-m)^2 T_m U_{n-m} + 2ACik^3 \sum\limits_{m=-\infty}^{\infty} m(n-m)^2 U_m T_{n-m} \\ \qquad -\dfrac{AC^2}{B}k^2 \sum\limits_{m=-\infty}^{\infty} (n-m)^2 T_m T_{n-m} + ABk^4 \sum\limits_{m=-\infty}^{\infty} m(n-m)^3 U_m U_{n-m} \\ \qquad -Bk^2 \sum\limits_{m=-\infty}^{\infty} m(n-m)V_m U_{n-m} - ACik \sum\limits_{m=-\infty}^{\infty} m V_m Q_{n-m} \\ \qquad -Cik \sum\limits_{m=-\infty}^{\infty} m V_m T_{n-m} \end{cases} \tag{4.22}$$

5. NUMERICAL ANALYSIS OF A COMBINED EFFECT OF THERMAL RELAXATION AND THERMOMECHANICAL COUPLING IN NONLINEAR DYNAMICS

In all numerical experiments reported in this section, we use the values of model parameters typical for polyisoprene [32]:

$$\begin{aligned}
&\rho_0 = 0.913(\mathrm{g/cm^3}) \qquad k_0 = 2,270\,(\mathrm{MPa}) = 2.27 \times 10^{10}\,(\mathrm{g/cm\,s^2}) \qquad \theta_0 = 293\,\mathrm{K} \\
&\mathcal{K} = 0.134\,\mathrm{W/m\,K} = 1.34 \times 10^4\,(\mathrm{g\,cm/s^3\,K}) \\
&\gamma = 11.8 \times 10^5\,\mathrm{N/m^2\,K} = 1.18 \times 10^7\,(\mathrm{g/cm\,s^2\,K}) \\
&\bar{c} = 1,905\,\mathrm{J/kg\,K} \times 0.913\,(\mathrm{g/cm^3}) = 1.74 \times 10^7\,(\mathrm{g/cm\,s^2\,K})
\end{aligned} \tag{5.1}$$

Substituting these values into (4.19), we obtain

$$x_* = 1.1 \times 10^{-9}\,\mathrm{cm} \qquad t_* = 6.9 \times 10^{-15}\,\mathrm{s}$$

In studying nonlinear dynamics of rubber-based polymeric materials with due regard to the effect of thermal relaxation, the fact that the time scale turns out to be very small is handy for the analysis of this dynamics. Indeed, note that the thermal relaxation time is also small, typically of the order of $10^{-15} - 10^{-12}$ s, depending on the material (see, e.g., [30, 34–37] and references therein). Since the value of t_* is less than or comparable to typical relaxation times, this will ensure the sensitivity of the model to fast processes in which the role of thermal relaxation cannot be ignored. The associated small value of x_* will allow us to resolve corresponding short spatial variations of thermal and mechanical fields.

However, care must be taken when dealing with the short spatial scales. Indeed, for fast and spatially short-scale processes, such as the second sound, the physical system is not in a state of local thermodynamic equilibrium and heat carriers should not obey any universal velocity distribution (e.g., Maxwell distribution). As a consequence, a difficulty arises in how to sensibly define the temperature, as it cannot be related to the kinetic energy of heat carriers averaged over some elementary space volume. At atomic length scales such volumes may even contain just one carrier, so that the averaging procedure loses sense. Traditionally, the elementary volume is assumed to have comparable extensions in all three dimensions (e.g., [38, 39] and references therein).

Our idea is to choose the initial conditions to the problem in such a way that the problem exhibits high frequency and short spatial distributions of temperature, leading to a situation in which thermal coupling and relaxation effects become important.

We define the temperature in a nontraditional way, designed specifically for extremely short quasi-one-dimensional waves like the second sound in elastic rings. The definition is similar to that originally proposed in [38] (see also [29]) in which temperature waves—waves of second sound—were studied. The authors of that article simulated the behavior of individual atoms in a three-dimensional lattice exposed to an initial heat pulse applied at the lattice end. The results were compared to available experimental data on NaF (e.g., [40]), and satisfactory correlation was

revealed at a qualitative level (see also a more recent article [40] and references therein). Note that in these experiments the lattice was supposed to be in thermal equilibrium initially, but the equilibrium was destroyed by the propagating heat wave. Under these conditions the kinetic temperature was introduced as the kinetic energy of atoms averaged over the cross-sectional lattice plane. Thus, the elementary volume was designed to have microscopic extension (comparable to atomic size) in the direction along the wave propagation but extended over many atomic sizes in the transverse direction. Due to the latter property, the elementary volume embraced many atoms; this allowed averaging over them when defining the temperature.

In the similar way, we define the temperature as the average kinetic energy of heat carriers over an elementary volume with extension of order x_* in the x direction (along the elastic ring) and of much greater extension in the transverse direction (across the ring). Having adopted this temperature definition, we view the CV equation as the model that well reproduces (although phenomenologically) main properties of the second sound, namely, finite propagation velocity and its wavy character.

The first group of experiments was set to demonstrate the influence of thermal relaxation on nonlinear dynamics of the polymeric body. We excited the ring thermally by introducing the initial temperature shown in Figure 2. Initial displacements and initial time derivatives of displacements and temperature are kept zero, so that we have

$$T(x,0) = R\left[1 + \frac{5}{2}\sin(kx)\right]^4 \qquad u(x,0) \equiv 0, \quad \left(\frac{\partial T}{\partial t}\right)_{t=0} \equiv 0, \quad \left(\frac{\partial u}{\partial t}\right)_{t=0} \equiv 0 \qquad (5.2)$$

The factor R in (5.2) is chosen so that the temperature at the maximum of the peak is equal to the melting temperature T_m of the polymeric material. For polyisoprene, $T_m = 35°\mathrm{C}$, consequently the corresponding nondimensional temperature equals 0.05, which is provided by $R = 10^{-3}/3$. Strictly speaking, once the initial conditions

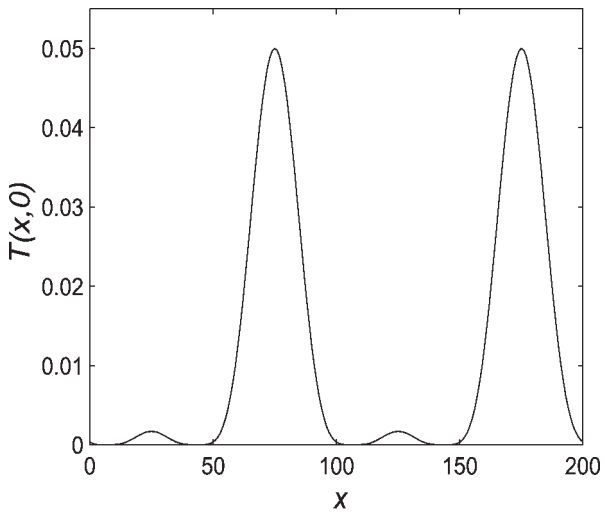

Figure 2. Initial temperature has the form of a peak.

are specified, we are left with the only free parameter in our model, namely, the wave number k. However, since the relaxation time is a parameter that is difficult to measure in practice and for most applications its value can be given within a specified range only, it is very instructive to conduct an experiment in which the influence of variations in this parameter on the nonlinear dynamics can be investigated. In what follows, we assume that the typical value of τ_0 for the materials under consideration is of the order $\tau_0 \approx 10^{-12}$ s.

We truncate the system (4.22) to a finite number of modes and integrate it in time using the fourth-order Runge-Kutta method. In our experiments we used typically 10 Fourier modes, which was sufficient to provide an accurate representation of the solution. Due to negligibly small contributions of higher modes to the solution of the problem, we observed practically the same profiles of computed thermomechanical fields when larger numbers of modes were used (up to 30).

In Figure 3 the dynamics of elongational oscillations are shown for $k = 1$ and $\tau_0 = 10^{-12}$ s. For convenience, all figures display two periods of temperature and displacement profiles [parts (*a*) and (*c*)]. Next to each 3-D plot we place the last recorded profile [(*b*) and (*d*), respectively]. Thus, the initial profile (Figure 2) and the profile computed at the last moment of time, t_1, are presented separately, while intermediate-time profiles can be judged based on the 3-D plots presented. The dynamics considered in this example are very irregular. Indeed, our computations beyond the chosen limiting moment t_1 showed that, eventually, nonlinear effects started to drive the profiles toward the formation of shock-type waves. The moment of shock-wave formation manifests itself by a typical rippling of displacement and temperature profiles, and therefore can be estimated computationally. In all our experiments we chose the limiting time t_1 small enough to avoid this phenomenon. The shock-wave formation in nonlinear thermoelasticity is a well-known phenomenon (especially in the context of classical models), which has been studied theoretically by a number of researchers (see, for example, [41]).

For smaller values of k representing a "stretched-out" initial temperature peak, a longer period is needed for the nonlinear terms to produce a noticeable effect. For example, Figure 4 ($k = 0.01$) shows the profiles [of temperature (Figure 4*a*) and of displacements (Figure 4*b*) formed by the moment $t_1 = 500$ when the peak changed substantially in height as compared to the initial profile. We found that even after such a relatively long evolution, the nonlinearities still have a negligible effect. This was confirmed by comparing the presented profiles with the profiles obtained with the linearized system (4.21). Another important observation that follows from Figure 4 is that the profiles corresponding to relaxation times smaller than 10^{-12} s practically coincide with each other. This is not surprising because, for sufficiently small values of τ_0, the terms with relaxation time [see (4.20)] practically vanish. We observe that the profile for a relatively large relaxation time corresponding to $\tau_0 = 10^{-11}$ s is clearly different from the other profiles, while the profile for $\tau_0 = 10^{-12}$ s is just slightly different from the profiles corresponding to smaller values of τ_0. Therefore, for given wave number $k = 0.01$, the relaxation time $\tau_0 = 10^{-12}$ s can be viewed as "critical" in the sense that one may expect an increasing influence of the effect of thermal relaxation for polymeric materials with larger values of τ_0. For larger wave numbers k, the nonlinear terms in the energy-balance equation play a significant role at earlier stages of the dynamics. Figure 5 shows profiles of the

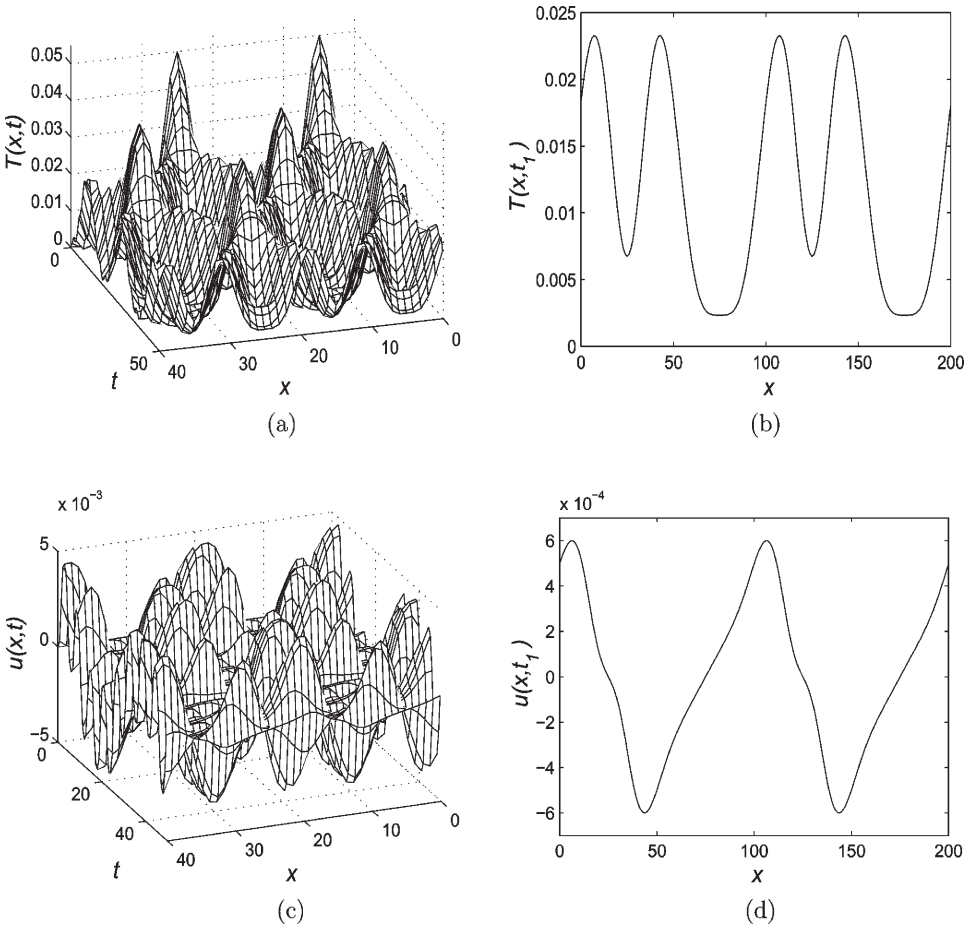

Figure 3. Dynamics of temperature and displacement ($t_1 = 50$).

thermal (Figure 5*a*) and mechanical (Figure 5*b*) fields for $k = 1$ at the moment $t_1 = 100$. The curves presented in this figure demonstrate distinctive difference between the results of computations with the full and the linearized system (4.21).

In the second group of experiments we investigated the combined effect of thermal relaxation and nonlinear oscillatory dynamics of the thermomechanical body. The main result is illustrated by Figure 6 ($k = 5$). First, note that the majority of the nonlinear terms in our system (4.20) contain the relaxation time parameter A. By switching from the case $\tau_0 = 10^{-12}$ s to the case $\tau_0 = 10^{-15}$ s, we decrease the value τ_0 and, consequently, suppress the nonlinearities. The first term on the right-hand side of the energy-balance equation [see (4.21)] becomes dominant, and we observe a damping of temperature, which leads eventually to its almost uniform spatial distribution (Figure 6*b*).Thereafter, displacements continue to oscillate, obeying, in essence, the usual wave equation of motion.

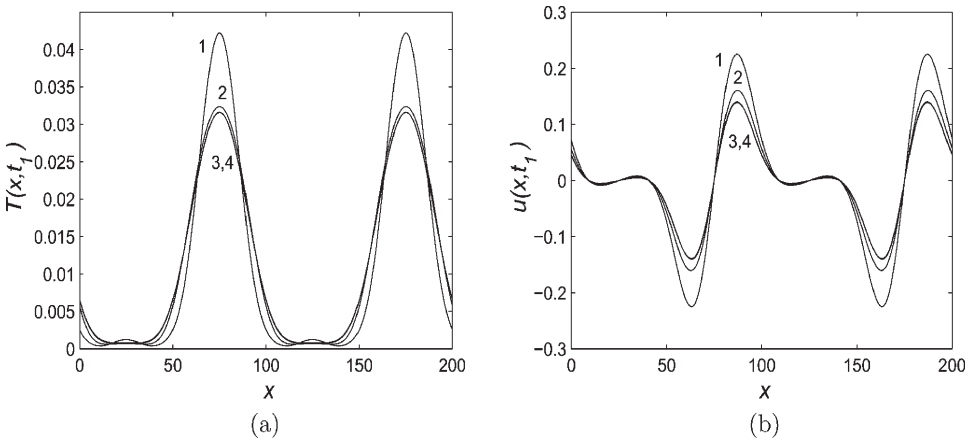

Figure 4. Temperature and displacement for different relaxation times: $\tau_0 = 10^{-11}$ s (1), 10^{-12} s (2), 10^{-13} s (3), 10^{-14} s (4).

This phenomenon should be viewed not only as a result of different roles of nonlinearities in the system, but as a combined effect of nonlinearities and thermal relaxation. Although we demonstrated the significance of this effect only for short spatial and temporal scales, it can be foreseen that the role of thermal relaxation can be far from negligible for larger scales. Indeed, the term containing the relaxation time, AC^2/B, makes a substantial contribution to the effective coefficient of temperature dissipation, $(B + AC^2/B)$. For the data (5.1), it can be easily found that $AC^2/B = 0.0026$ and $B = 0.00076$. Although this estimate is pretty rough, it clearly points out to the possibility for the ratio AC^2/B to become appreciable compared to the value of B, even though the value of τ_0 remains small.

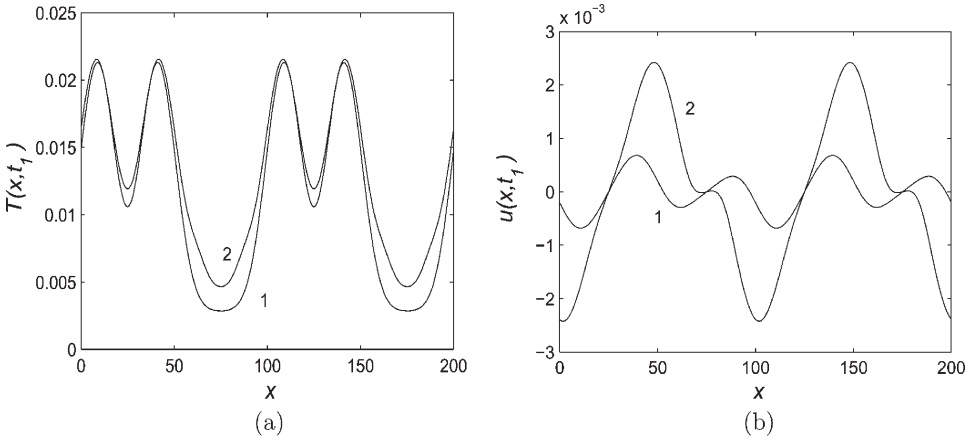

Figure 5. Temperature and displacement obtained with the linear (1) and nonlinear (2) system. $\tau_0 = 10^{-12}$ s.

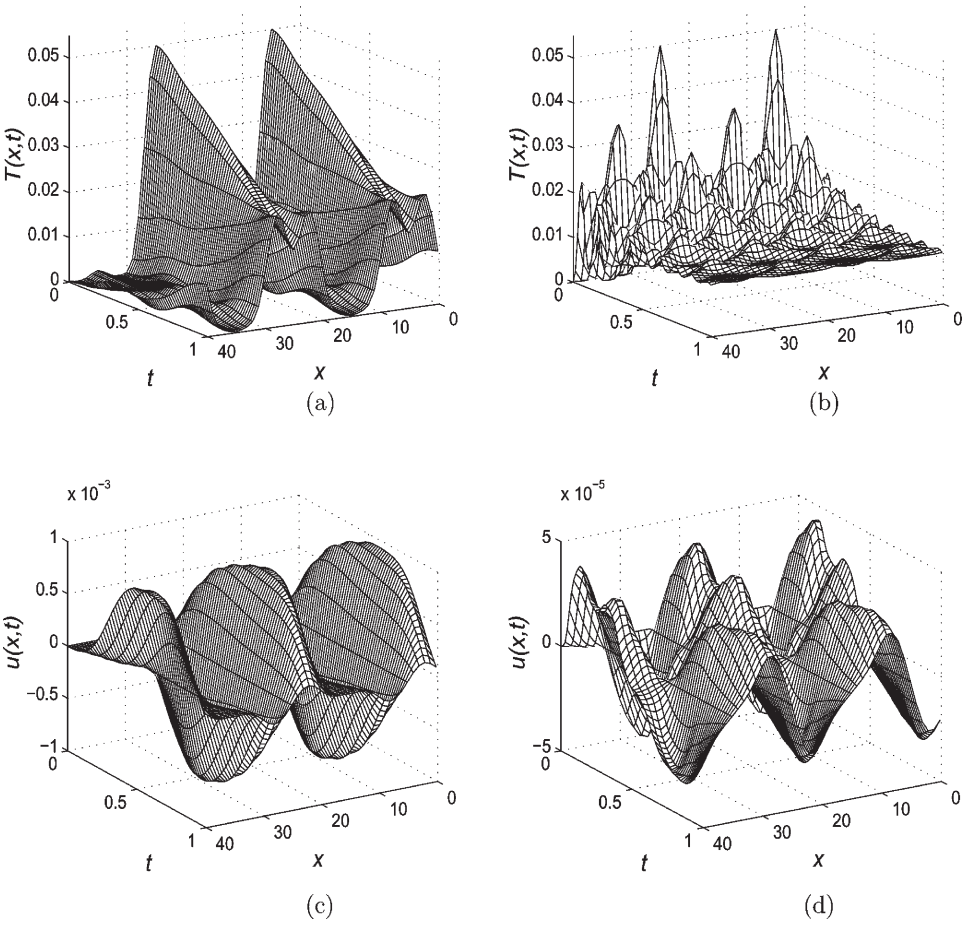

Figure 6. Dynamics of temperature and displacement for $\tau_0 = 10^{-12}$ s (left column) and $\tau_0 = 10^{-15}$ s (right column).

6. CONCLUSIONS

Using computer simulation, we studied the thermomechanical behavior of rubber-based polymeric materials, with special attention given to the role of the thermal relaxation phenomenon in nonlinear dynamics. We considered elongational oscillations of a ring-shaped body, which provided us with an instructive example for studying important features of a combined effect of thermal relaxation and thermomechanical coupling. We derived a nonlinear thermomechanical model based on conventional forms of free-energy functions for these polymeric materials and the Cattaneo-Vernotte equation allowing for the effect of thermal relaxation. The model comprising the equations of motion and energy balance represents a generalization of the classical Lord-Schulman model, and in the linear case the two models are identical. A distinctive feature of our model is its ability to allow for a combined effect of thermal relaxation and nonlinear character of oscillatory dynamics of

the thermomechanical system. This effect is most pronounced for high time frequency and short spatial variations of temperature and displacements. This case was analyzed numerically with a computational scheme based on the Fourier decomposition of thermomechanical fields. Since most of nonlinear terms in our model contain the thermal-relaxation time parameter, we conducted a series of numerical experiments to reveal a close connection between nonlinear dynamics of the system and the phenomenon of thermal relaxation. In particular, we demonstrated that vanishing relaxation time can lead to a remarkable damping of nonlinear effects in the dynamics of the thermomechanical system.

REFERENCES

1. G. Rabilloud, *High Performance Polymers: Chemistry and Applications*, Editions Technip, Paris, 1999.
2. D. S. Chandrasekharaiah, Hyperbolic Thermoelasticity: A Review of Recent Literature, *Appl. Mech. Rev.*, vol. 51, pp. 705–729, 1998.
3. R. B. Hetnarski and J. Ignaczak, Soliton-like Waves in a Low-Temperature Nonlinear Thermoeleastic Solid, *Int. J. Eng. Sci.*, vol. 34, pp. 1767–1787, 1996.
4. K. Saxton, R. Saxton, and W. Kosinski, On Second Sound at the Critical Temperature, *Quart. Appl. Math.*, vol. LVII, pp. 723–740, 1999.
5. D. V. Strunin, R. V. N. Melnik, and A. J. Roberts, Coupled Thermomechanical Waves in Hyperbolic Thermoelasticity, *J. Thermal Stresses*, vol. 24, no. 2, pp. 121–140, 2001.
6. R. V. N. Melnik, Discrete Models of Coupled Dynamic Thermoelasticity for Stress-Temperature Formulations, *Appl. Math. Comput.*, vol. 122, no. 1, pp. 107–132, 2001.
7. L. R. G. Treloar, *The Physics of Rubber Elasticity*, Clarendon Press, Oxford, 1975.
8. R. W. Ogden, *Non-linear Elastic Deformations*, Wiley, New York, 1984.
9. C. Miehe, Entropic Thermoelasticity at Finite Strains. Aspects of the Formulation and Numerical Implementation, *Comput. Meth. Appl. Mech. Eng.*, vol. 120, pp. 243–269, 1995.
10. G. A. Holzapfel and J. C. Simo, Entropy Elasticity of Isotropic Rubber-like Solids at Finite Strains, *Comput. Meth. Appl. Mech. Eng.*, vol. 132, pp. 17–44, 1996.
11. S. Reese and S. Govindjee, Theoretical and Numerical Aspects in the Thermo-Viscoelastic Material Behaviour of Rubber-like Polymers, *Mech. Time-Dependent Mater.*, vol. 1, pp. 357–396, 1998.
12. K.-D. Papoulia, Mixed and Selective Integration Procedures in Large Strain Hyperelastic Analysis of Nearly Incompressible Solids, *Comput. Mech.*, vol. 23, pp. 63–74, 1999.
13. P. Le Tallec, *Numerical Analysis of Viscoelastic Problems*, Masson, Paris, 1990.
14. P. M. Morse and H. Feshbach, *Methods of Theoretical Physics*, McGraw-Hill, New York, 1953.
15. M. Renardy, W. J. Hrusa, and J. A. Nohel, *Mathematical Problems in Viscoelasticity*, Longman, New York, 1987.
16. J. C. Simo and T. J. R. Hughes, *Computational Inelasticity*, Springer-Verlag, Berlin, New York, 1998.
17. R. Schirrer, C. Fond, and A. Lobbrecht, Volume Change and Light Scattering during Mechanical Damage in Polymethylmethacrylate Toughened with Core-Shell Rubber Particles, *J. Mater. Sci.*, vol. 31, pp. 6409–6422, 1996.
18. Y. Yokoyama and T. Ricco, Toughening of Polypropylene by Different Elastomeric Systems, *Polymer*, vol. 39, pp. 3675–3681, 1998.
19. Y. C. Gao and T. Gao, Mechanical Behaviour of Two Kinds of Rubber Materials, *Int. J. Solids Struct.*, vol. 36, pp. 5545–5558, 1999.
20. M. E. Gurtin, *An Introduction to Continuum Mechanics*, Academic, New York, 1981.

21. S. R. Bodner and M. B. Rubin, A Unified Elastic-Viscoplastic Theory with Large Deformations, in J. Gittus, J. Zarka, and S. Nemat-Nasser (eds.), *Large Deformations of Solids: Physical Basis and Mathematical Modelling*, pp. 129–140, Elsevier Applied Science, London, 1996.
22. J. C. Slattery, *Advanced Transport Phenomena*, Cambridge University Press, Cambridge, 1999.
23. P. Chadwick, Thermo-mechanics of Rubberlike Materials, *Phil. Trans. Roy. Soc. Lond.*, vol. A276, pp. 371–403, 1974.
24. G. A. Holzapfel, Physical Modeling and Finite Element Analysis in Rubber Thermoelasticity. *Z. Angew. Math. Mech.*, vol. 78, no. S1, pp. S133–S136, 1998.
25. S. Doll, K. K. Schweizerhof, R. Hauptmann, and C. Freischlager, On Volumetric Locking of Low-Order Solid and Solid-Shell Elements for Finite Elastoviscoplatic Deformations and Selective Reduced Integration, *Eng. Comput.*, vol. 17, no. 7, pp. 874–902, 2000.
26. A. Ionita, Finite Element Analysis of the Deformation of a Rubber Diaphragm, Ph.D. Thesis, Virginia PISU, Blacksburg, 2001.
27. R. W. Penn, Volume Changes Accompanying the Extension of Rubber, *Trans. Soc. Rheol.*, vol. 14, pp. 509–517, 1970.
28. W. Nowacki, *Dynamic Problems of Thermoelasticity*, Noordhoff, Leyden, The Netherlands, 1975.
29. D. Potter, *Computational Physics*, Wiley, London, 1973.
30. D. D. Joseph and L. Preziosi, Heat Waves, *Rev. Mod. Phys.*, vol. 61, pp. 41–73, 1989.
31. D. Y. Tzou, Thermal Control in Solids with Rapid Relaxation, *J. Dynam. Measure. Control*, vol. 125, pp. 563–568, 2003.
32. L. D. Landau and E. M. Lifshitz, *Theory of Elasticity*, Butterworth-Heinemann, Oxford, Boston, 1995.
33. J. Brandrup, E. H. Immergut, and E. A. Grulke (eds.), *Polymer Handbook*, Wiley, New York, 1999.
34. H. W. Lord and Y. Schulman, A Generalized Dynamic Theory of Thermoelasticity, *J. Mech. Phys. Solids*, vol. 15, pp. 299–309, 1967.
35. C. S. Suh and C. P. Burger, Effects of Thermomechanical Coupling and Relaxation Times on Wave Spectrum in Dynamic Theory of Generalized Thermoelasticity, *J. Appl. Mech.*, vol. 65, pp. 605–613, 1998.
36. P. Poelt, E. Ingolic, M. Gahleither, K. Bernreitner, and W. Geymayer, Characterization of Modified Polypropylene by Scanning Electron Microscopy, *J. Appl. Polymer Sci.*, vol. 78, pp. 1152–1161, 2000.
37. D. S. Chandrasekharaiah, Thermoelasticity with Second Sound: A Review, *Appl. Mech. Rev.*, vol. 39, pp. 355–376, 1986.
38. Thermo-mechanical Effects in Elastic Wave Propagation: A Survey, *J. Sound Vib.*, vol. 21, pp. 181–192, 1972.
39. D. H. Tsai and R. A. MacDonald, Molecular-Dynamical Study of Second Sound in a Solid Excited by a Strong Heat Pulse, *Phys. Rev. B*, vol. 14, pp. 4714–4723, 1976.
40. J. R. Ho, C. P. Kuo, W. S. Jiaung, and C. J. Twu, Lattice Boltzmann Scheme for Hyperbolic Heat Conduction Equation, *Numer. Heat Transfer B*, vol. 41, pp. 591–607, 2002.
41. T. F. McNelly, S. J. Rogers, D. J. Channin, R. J. Rollefso, W. M. Goubau, G. E. Schmidt, J. A. Krumhans, and R. H. Pohl, Heat Pulses in NaF: Onset of Second Sound, *Phys. Rev. Lett.*, vol. 24, pp. 100–102, 1970.
42. R. Racke, Blow-up in Non-linear Three-Dimensional Thermoelasticity, *Math. Meth. Appl. Sci.*, vol. 12, pp. 267–273, 1990.